Preprocessing with Image Denoising and Histogram Equalization for Endoscopy Image Analysis Using Texture Analysis

Tomoyuki Hiroyasu[1], Katsutoshi Hayashinuma[2], Hiroshi Ichikawa[1] and Nobuaki Yagi[3]

***Abstract*— A preprocessing method for endoscopy image analysis using texture analysis is proposed. In a previous study, we proposed a feature value that combines a co-occurrence matrix and a run-length matrix to analyze the extent of early gastric cancer from images taken with narrow-band imaging endoscopy. However, the obtained feature value does not identify lesion zones correctly due to the influence of noise and halation. Therefore, we propose a new preprocessing method with a non-local means filter for de-noising and contrast limited adaptive histogram equalization. We have confirmed that the pattern of gastric mucosa in images can be improved by the proposed method. Furthermore, the lesion zone is shown more correctly by the obtained color map.**

I. INTRODUCTION

Gastric cancer is the fifth most common cancer in the world and the third leading cause of cancer death [1]. Gastric cancer can be cured by early detection and treatment. Recently, narrow-band imaging (NBI) endoscopy has drawn attention as a diagnostic method for gastric cancer. Using NBI endoscopy, the structure of the mucosa and the vascular structure of the stomach can be observed clearly. Findings indicate that the microsurface pattern and microvascular pattern of a lesion zone of an NBI image are lossy, uneven, or asymmetric [2]. Currently, diagnosis of the lesion zone is performed by visual observation. However, it is possible to make a false diagnosis because there is no quantitative index for this diagnosis.

Therefore, computer-aided diagnosis (CAD) for endoscopy images is performed to facilitate diagnoses. Riaz et al. performed the classification of endoscopy images using the Gabor filter or a local binary pattern (LBP) [3], [4]. In addition, Tamaki et al. performed classification of endoscopy images using scale invariant feature transform (SIFT) [5]. However, the purpose of these studies was not to evaluate the extent of a lesion zone but to classify an image. Lee et al. and Chen et al. detected the lesion zone using a LBP or a gray level co-occurrence matrix (GLCM) [6], [7]. Endoscopic images have significant diversity; therefore, it is not realistic to prepare a sufficient number of training images. Consequently, a method that does not employ training images is required.

[1]T. Hiroyasu and H. Ichikawa are with the Faculty of Life and Medical Science, Doshisha University, Kyoto, Japan
tomo@is.doshisha.ac.jp
hichikawa@mail.doshisha.ac.jp
[2]K. Hayashinuma is with the Graduate School of Life and Medical Science, Doshisha University, Kyoto, Japan
khayashinuma@mis.doshisha.ac.jp
[3]N. Yagi is with the Department of Gastroenterology, Murakami Memorial Hospital, Asahi University, Gifu, Japan
nyagi@koto.kpu-m.ac.jp

To satisfy this need, we have previously proposed an analysis using a GLCM and a gray level run-length matrix (GLRM) [8]. However, lighting conditions were not considered in that method. As a result, dark shadowed regions are noisy, and the feature values are greatly changed around halation. To solve these problems, we propose a new preprocessing method with contrast enhancement using contrast limited adaptive histogram equalization (CLAHE) [9] after de-noising using a non-local means filter [10].

II. ENDOSCOPY IMAGE ANALYSIS METHOD USING GLCM AND GLRM

We have previously proposed a method of analyzing endoscopy images using a feature value with the image [8]. In that method, the input image is transformed into grayscale. Subsequently, windows are scanned in an image reduced to 16 colors, and correlation (COR) from the GLCM and gray level non-uniformity (GLN) from the GLRM are calculated for each window. An endoscopy image is analyzed using a feature value obtained by combining COR and GLN.

GLCM consists of $P_{(r,\theta)}(i,j)$, i.e., the probabilities that the gray level of the pixel is j when that pixel appears at a distance of r at an angle of θ from a pixel with a gray level of i. In this study, angle θ is used at $0^\circ, 45^\circ, 90^\circ$ and 135°. Haralick et al. proposed determination of 14 feature values [11]. COR are calculated as follows.

$$\mathrm{COR} = \frac{\sum_{i=0}^{n-1}\sum_{j=0}^{n-1} i\cdot j P_{(r,\theta)}(i,j) - \mu_x \cdot \mu_y}{\sigma_x \cdot \sigma_y} \tag{1}$$

Here,

$$\mu_x = \sum_{i=0}^{n-1}\left\{ i \sum_{i=0}^{n-1} P_{(r,\theta)}(i,j)\right\} \tag{2}$$

$$\mu_y = \sum_{j=0}^{n-1}\left\{ j \sum_{j=0}^{n-1} P_{(r,\theta)}(i,j)\right\} \tag{3}$$

$$\sigma_x^2 = \sum_{i=0}^{n-1}\left\{ (i-\mu_x)^2 \sum_{i=0}^{n-1} P_{(r,\theta)}(i,j)\right\} \tag{4}$$

$$\sigma_y^2 = \sum_{j=0}^{n-1}\left\{ (j-\mu_y)^2 \sum_{j=0}^{n-1} P_{(r,\theta)}(i,j)\right\} \tag{5}$$

This represents the correlation of a combination of gray levels. In an endoscopy image, the COR value in an observed lesion zone tends to be low.

In contrast, the GLRM represents the length of the series of pixels with the same gray level within the pixels aligned in a given direction. This is denoted $P_\theta(i,j)$, i.e., the same gray

978-1-4244-9270-1/15/$31.00 ©2015 IEEE

level of i is j pixels continuous in the direction of angle θ. In this study, angle θ is used at $0°, 45°, 90°$ and $135°$. Galloway proposed determination of five feature values from such a matrix [12]. The GLN is calculated as follows.

$$\mathrm{GLN} = \frac{1}{T}\sum_{i=0}^{g-1}\left[\sum_{j=1}^{N} P_\theta(i,j)\right]^2 \tag{6}$$

Here,

$$T = \sum_{i=0}^{g-1}\sum_{j=1}^{N} P_\theta(i,j) \tag{7}$$

This GLN represents the deviation of the gray level. In an endoscopy image, the GLN value in a lesion zone tends to be high.

In this study, COR and GLN are integrated for each angle and further integrated to a single feature value based on the combined values. COR and GLN are integrated for each angle as follows.

$$F_\theta = (1 - \mathrm{COR}_\theta) \times \mathrm{GLN}_\theta \tag{8}$$

Since COR is lower and GLN is higher in the lesion zone, the feature value is formulated to exhibit a high value in the lesion zone. Next, the combined feature values in each angle are integrated to a single feature value based on the gradient ratio. The gradient strength $m(u,v)$ and gradient direction $\theta(u,v)$ in image I are calculated as follows.

$$m(u,v) = \sqrt{f_u(u,v)^2 + f_v(u,v)^2} \tag{9}$$

$$\theta(u,v) = \tan^{-1}\frac{f_v(u,v)}{f_u(u,v)} \tag{10}$$

Here,

$$f_u(u,v) = \mathrm{I}(u+1,v) - \mathrm{I}(u-1,v) \tag{11}$$

$$f_v(u,v) = \mathrm{I}(u,v+1) - \mathrm{I}(u,v-1) \tag{12}$$

These gradient directions are quantized to eight directions. Subsequently, the ratio of gradient direction h_θ is calculated as follows.

$$h_\theta = \frac{\sum m_\theta(u,v)}{\sum_\theta m_\theta(u,v)} \tag{13}$$

At this time, gradient directions of $180°$, $225°$, $270°$ and $315°$ are considered as $0°$, $45°$, $90°$ and $135°$, respectively. A new feature value F is integrated by multiplying F_θ and h_θ.

$$F = \sum_\theta F_\theta \cdot h_\theta \tag{14}$$

Using this feature value, the lesion zone is presented by creating a color map.

The analyzed result obtained by this method is shown in Fig. 1. Fig. 1(a) shows an image taken with NBI endoscopy. Here, the dashed line is the demarcation line. Fig. 1(b) shows the result of the color map for the endoscopy image. It is possible to read the lesion zone from the color map. However, the shadowed region is emphasized more than the lesion zone. In addition, the feature value decreased greatly around halation. These changes are because the continuity

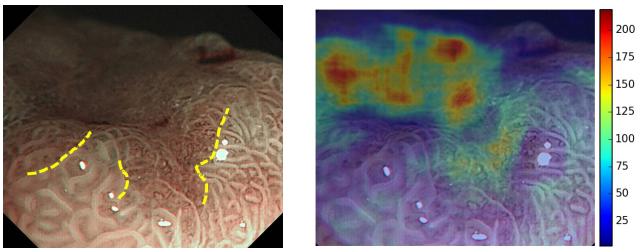

(a) (b)

Fig. 1. Results of a previous method: (a) input image; (b) color map

of the pixels changed significantly from those of the mucosa relative to noise or halation. In the next section, we propose a preprocessing method to solve these problems.

III. Preprocessing with De-noising and Histogram Equalization

To solve the problem mentioned in the previous section, we propose a preprocessing method. In the proposed preprocessing method, CLAHE is applied as contrast emphasis after de-noising using a non-local means filter.

The non-local means filter was proposed for image denoising by Buades et al. [10]. In this method, noise was reduced, i.e., the value of the pixel of interest was replaced by the weighted average of reference pixels depending on the similarity of the block centered on the pixel of interest and the reference pixel. When $x(i)$ corresponds to the pixel of interest in image I, $w(i,j)$ corresponds to the weight and $s(i,j)$ corresponds to the similarity of the block of interest and the reference block. The pixel value $y(I,j)$ after denoising is expressed as follows.

$$y(i) = \sum_{j\in I} w(i,j)x(i,j) \tag{15}$$

$$w(i,j) = \frac{s(i,j)}{\sum_{l\in I} s(i,l)} \tag{16}$$

$$s(i,j) = \exp\left(-\frac{\|\boldsymbol{v}(i) - \boldsymbol{v}(j)\|^2}{h^2}\right) \tag{17}$$

Here, $v(j)$ is a two-dimensional vector obtained by arranging pixel values in the block of $k \times k$ around pixel i. h is a parameter that determines the strength of smoothing.

CLAHE is a histogram equalization method proposed by Pizer et al. [9]. We have used adaptive histogram equalization because the brightness changes significantly in an endoscopy image. First, the image is divided into equal-sized areas that do not overlap. Next, a histogram is computed for each region. Finally, the histogram is clipped, and the clipped value is distributed after histogram equalization.

IV. Experiment

A. Outline of the experiment

In this experiment, we used an early gastric cancer image taken using NBI endoscopy at the Murakami Memorial Hospital. A color map was derived by applying the proposed

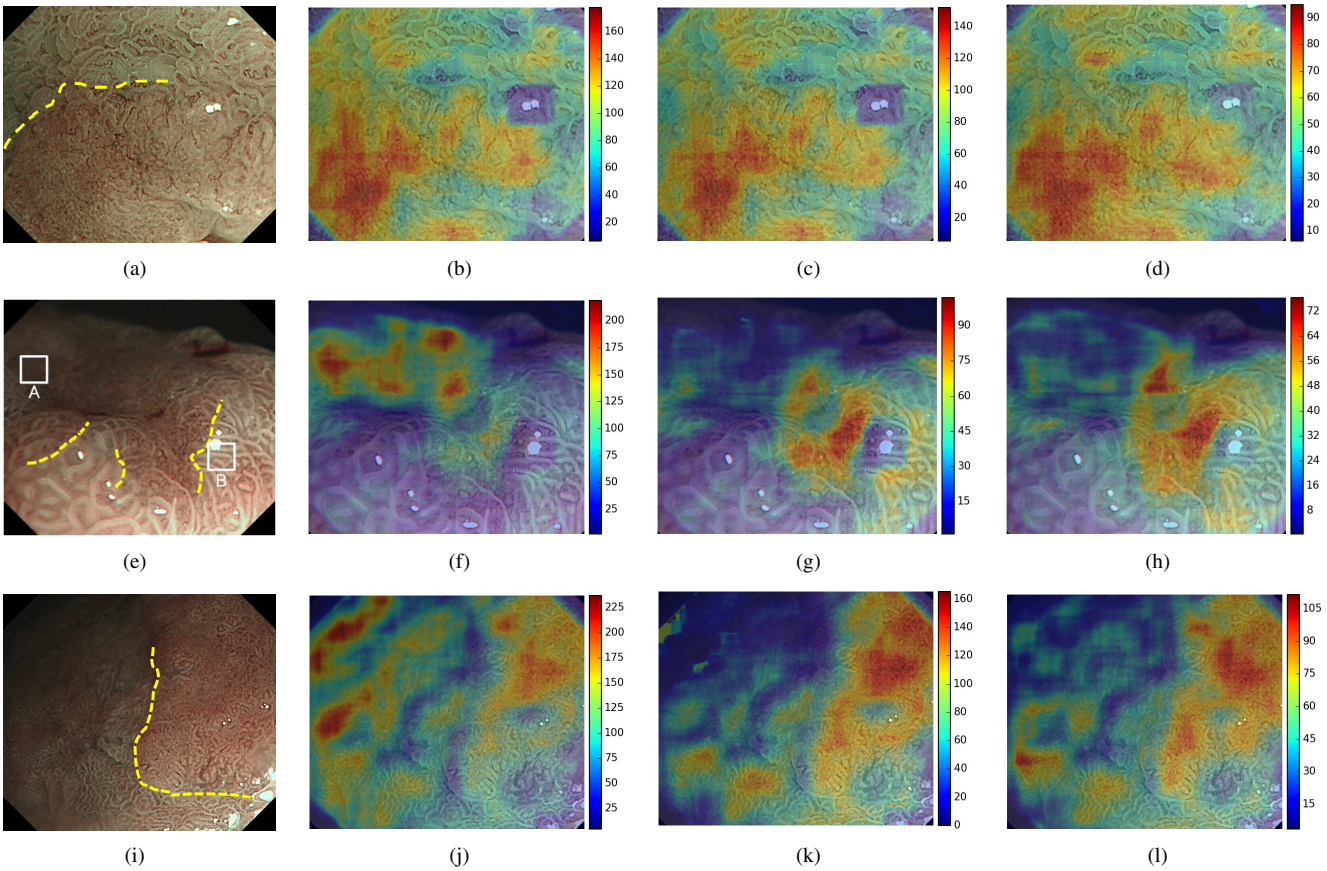

Fig. 2. Experimental results. (a)(e)(i): input images, (b)(f)(j): color maps (without preprocessing), (c)(g)(k): color maps (with non-local means filter), (d)(h)(l): color maps (with non-local means filter and CLAHE)

method. We compared the results obtained without preprocessing, with only de-noising, and with contrast emphasis after de-noising. The image size was 850×736 [pixel]. The window size used to obtain the feature value was 100×100 [pixel]. The block size of de-noising with the non-local means filter was 7×7 [pixel], and the search window size was 21×21 [pixel]. The tile size contrast enhancing with CLAHE was 8×8 [pixel]. The maximum value was shown in red, and the minimum value was shown in blue in each color map.

B. Experimental results

The input images and color maps are shown in Fig. 2. The color maps include images without preprocessing, with only de-noising, and with contrast emphasis after de-noising.The dashed line in the input image is the demarcation line between the lesion and the normal zone drawn by the doctor.

We compared the results obtained without preprocessing and the results with de-noising using the non-local means filter. The feature value was reduced in the entire region. In particular, the feature value in the shadowed region was greatly reduced (Fig. 2(g), (k)). Since the feature value in the shadowed region was very large, most of the red region in the color map was the shadowed region. By decreasing this, the feature value of region of interest is shown on the color map. Next, we compared the results obtained with de-noising and the results obtained with de-noising and contrast enhancement with CLAHE. It was observed that the feature value increased around the halation (Fig. 2(d), (h)).

Changes in COR and GLN values by preprocessing in the shadowed area (region A in Fig. 2(e)) and the area around the halation (region B in Fig. 2(e)) are shown in Fig. 3. As can be seen, COR increased and GLN decreased in the shadowed area by de-noising. In contrast, the GLN increased in the halation area by contrast enhancement. In addition, the enlarged image of regions A and B are shown in Fig. 4 and Fig. 5, respectively. In region A, particulate noise was lost by de-noising. It is assumed that the GLN was decreased by de-noising because it took a large value when there were many short runs in the same pixel value. In addition, it is assumed that COR increased by de-noising because it represents the correlation of pairs of pixel values and a pair with the same gray level was increased. On the other hand, the pattern of gastric mucosa was reinforced by contrast enhancement. The pattern of gastric mucosa was recognized correctly, and this may increase the value of GLN.

V. CONCLUSION

In this paper, we have proposed a preprocessing method to remove noise that appears when analyzing images of early gastric cancer taken with NBI endoscopy using a GLCM

and a GLRM. In the proposed method, de-noising with non-local means filter and contrast enhancing with CLAHE was performed with an endoscopy image. To examine the effectiveness of the proposed method, we performed an experiment. The results of de-noising indicate that the feature value was decreased at noisy shadowed areas. In addition, the results of contrast enhancement indicate that the feature value increased around the halation area. Thus, the lesion zone was emphasized effectively in the color map. As a result, our analysis of the endoscopy images using texture analysis has confirmed that preprocessing with a non-local means filter for de-noising and CLAHE for contrasting emphasis is effective. In future, we intend to consider the parameters of the non-local means filter and CLAHE to enhance accuracy.

REFERENCES

[1] "GLOBCAN 2012 Stomach Cancer Estimated Incidence, Mortality and Prevalence Worldwide in 2012," http://globocan.iarc.fr/Pages/fact_sheets_cancer.aspx.

[2] K. Yao, G. Anagnostopoulos, and K. Ragunath, "Magnifying endoscopy for diagnosing and delineating early gastric cancer," *Endoscopy*, vol. 41, no. 5, pp. 462–467, 2009.

[3] F. Riaz, F. Silva, M. Ribeiro, and M. Coimbra, "Invariant gabor texture descriptors for classification of gastroenterology images," *IEEE Transactions on Biomedical Engineering*, vol. 59, no. 10, pp. 2893–2904, 2012.

[4] F. Riaz, M. Ribeiro, P. Pimentel-Nunes, and M. Coimbra, "Integral Scale Histogram Local Binary Patterns for Classification of Narrow-band Gastroenterology Images," in *2013 35th Annual International Conference of the IEEE Engineering in Medicine and Biology Society (EMBC)*, Osaka, Japan, 2013, pp. 3714–3717.

[5] T. Tamaki, J. Yoshimuta, M. Kawakami, B. Raytchev, K. Kaneda, S. Yoshida, Y. Takemura, K. Onji, R. Miyaki, and S. Tanaka, "Computer-aided colorectal tumor classification in nbi endoscopy using local features," *Medical Image Analysis*, vol. 17, no. 1, pp. 78–100, 2013.

[6] T. Lee, Y. Lin, N. Uedo, H. Wang, H. Chang, and C. Hung, "Computer-aaided diagnosis in endoscopy: A novel application toward automatic detection of abnormal lesions on magnifying narrow-band imaging endoscopy in the stomach," in *2013 35th Annual International Conference of the IEEE Engineering in Medicine and Biology Society (EMBC)*, Osaka, Japan, 2013, pp. 4430–4433.

[7] Y. Chen, N. Uedo, J. Lee, T. Kanesaka, T. Lee, H. Wang, and H. Chang, "Detection and classification aof abnormal lesions in magnified nbi endoscopy images of stomach using gray level co-occurrence matrix method," in *The 2015 Joint Conference of the International Workshop on Advanced Image Technology (IWAIT) and the International Forum on Medical Imaging in Asia (IFMIA)*, Tainan, Taiwan, 2015, pp. 1–4.

[8] T. Hiroyasu, K. Hayashinuma, H. Ichikawa, N. Yagi, and U. Yamamoto, "Endoscope image analysis method for evaluating the extent of early gastric cancer," in *2014 IEEE Symposium on Computational Intelligence for Multimedia, Signal and Vision Processing (CIMSIVP)*, Orlando, USA, 2014, pp. 30–35.

[9] S. Pizer, E. Amburn, J. Austin, R. Cromartie, A. Geselowitz, T. Greer, B. Romeny, and J. Zimmerman, "Adaptive histogram equalization and its variations," *Computer Vision Graphics, and Image Processing*, vol. 39, no. 3, pp. 355–368, 1987.

[10] A. Buades, B. Coll, and J. Morel, "A non-local algorithm for image denoising," in *2005 IEEE Computer Society Conference on Computer Vision and Pattern Recognitio (CVPR)*, vol. 2, San Diego, USA, 2005, pp. 60–65.

[11] R. Haralick, K. Shanmugam, and I. Dinstein, "Textural Features for Image Classification," *IEEE Transactions on Systems, Man and Cybernetics*, vol. SMC-3, no. 6, pp. 610–621, 1973.

[12] M. Galloway, "Texture analysis using gray level run lengths," *Computer Graphics and Image Processing*, vol. 4, no. 2, pp. 172–179, 1975.

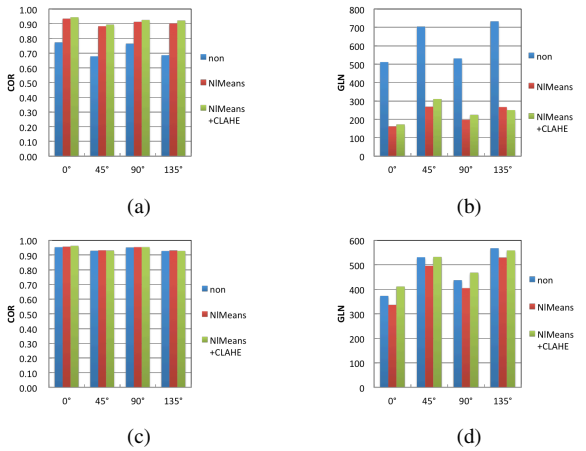

Fig. 3. Change of COR and GLN. (a) COR of shadowed area, (b) GLN of shadowed area, (c) COR of halation area, (d) GLN of halation area

Fig. 4. Region A after reduced color. (a) without preprocessing, (b) with non-local means filter, (c) with non-local means filter and CLAHE

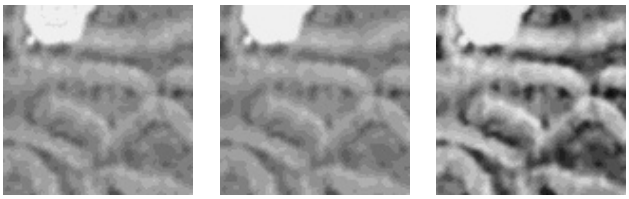

Fig. 5. Region B after reduced color. (a) without preprocessing, (b) with non-local means filter, (c) with non-local means filter and CLAHE